TURBINE ENGINE MATERIALS DURABILITY RESEARCH

S. R. Levine and C. A. Stearns
NASA Lewis Research Center
Cleveland, Ohio

INTRODUCTION

Turbine engine hot-section materials are subjected to aggressive chemical and thermomechanical environments. High-temperature environmental attack of dollar-intensive turbine components reduces turbine efficiency and can limit life. The bottom line, of course, is that high-temperature environmental attack costs you money. The objective of materials durability research at Lewis is to understand the mechanisms of alloy and coating attack and the effects of interaction with the environment on mechanical behavior. This base of understanding provides the foundation for developing life prediction methods and identifying strategies for controlling attack.

The major thrusts of our research can be grouped into the categories of environmental attack and control strategies or surface protection. Under environmental attack, which encompasses environmental effects on mechanical properties, we are concerned with oxidation attack, hot corrosion attack and life prediction. In the surface protection area, our major thrusts have been metallic coatings and ceramic thermal barrier coatings, and to these we have recently added a new area of research - coatings for carbon-carbon composites. Rather than skimming over all of these areas, this paper will cover only two areas - oxidation research and thermal barrier coating research. This will exemplify our philosophy while providing some depth of coverage for each topic. Recent reviews of the other areas of research are available (1-3).

SCHEMATIC VIEWS OF SURFACES OF OXIDIZED METALS

Three oxidation cases, as illustrated in figure 1, are of concern when dealing with the oxidation of nickel-base and cobalt-base superalloys and the coatings one might use to protect these materials at high temperature. Protection is derived from the ability to form an adherent, slowly growing oxide scale. The parabolic oxidation case is primarily of academic interest since it is rarely observed in cyclic oxidation. The systems that display this behavior generally form oxides that grow too rapidly to be useful as high-temperature protective scales, such as nickel oxide. Chromium oxide is another commonly encountered high-temperature oxide scale. This oxide is desirable under static conditions since it is generally tenacious and grows more slowly than nickel oxide. However, Cr_2O_3 undergoes oxidative vaporization in a high-temperature, high-velocity environment and this limits its utility. The final case, that of spalling, is exemplified by aluminum oxide and spinels. These oxides grow relatively slowly, do not vaporize, and only exhibit partial spallation. Thus, they have proven to be the most desirable protective scales for superalloys and their coatings.

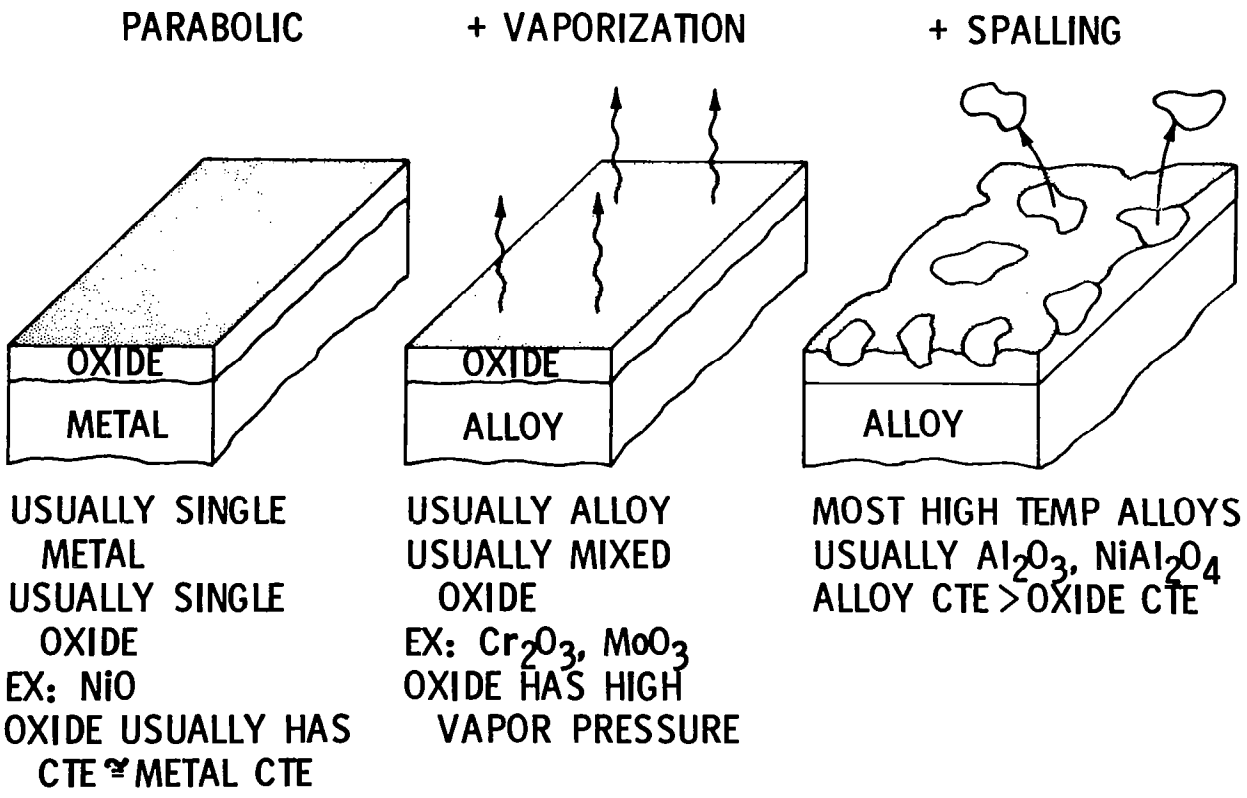

Figure 1

TYPES OF OXIDATION BEHAVIOR

Qualitative examples of the cyclic oxidation curves one might see with the three cases just discussed are illustrated in figure 2. The parabolic case, e.g. NiO, can be characterized by the parabolic rate constant, k_p. For an oxide which grows parabolically, but has a relatively high vapor pressure, such as Cr_2O_3, the linear vaporization constant, k_v, must be used in addition to k_p. For a system where the oxide grows parabolically, vaporizes at temperature, and partially spalls after each thermal cycle, the oxidation curve becomes quite complicated. However, the dashed curve gives an adequate representation and this involves a second linear constant, k_s, to account for spalling.

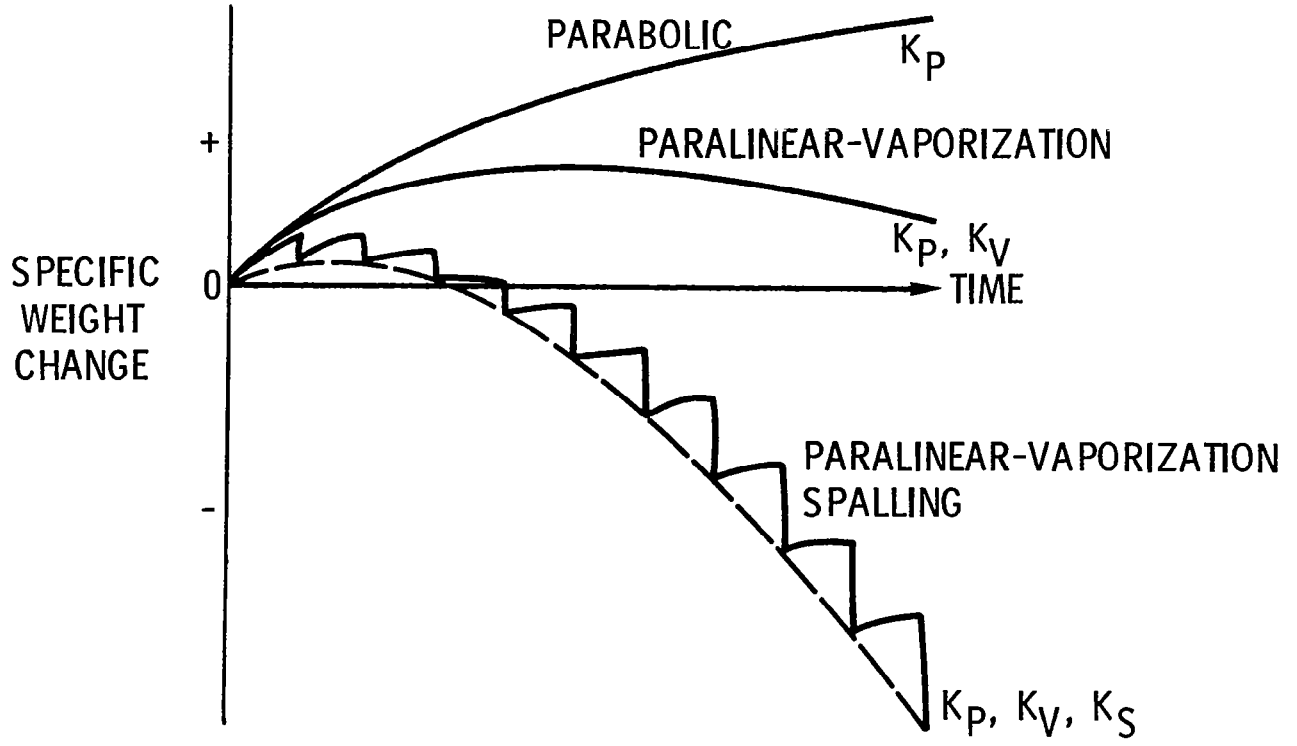

Figure 2

FUNDAMENTALS OF PROTECTIVE Al_2O_3 GROWTH

Because of the technological importance of aluminum oxide as a high-temperature protective scale, extensive studies of its growth behavior and morphology have been carried out (4). As a result it has been postulated, based on morphological evidence from the oxide scale-metal interface, that alumina grows most rapidly via grain boundary diffusion. This model has been verified by measurements of k_p as a function of grain size. The fact that large grain scales grow more slowly holds forth the promise for improving the protective capability of alumina scales through microstructural control (J. L. Smialek, unpublished research). (See fig. 3.)

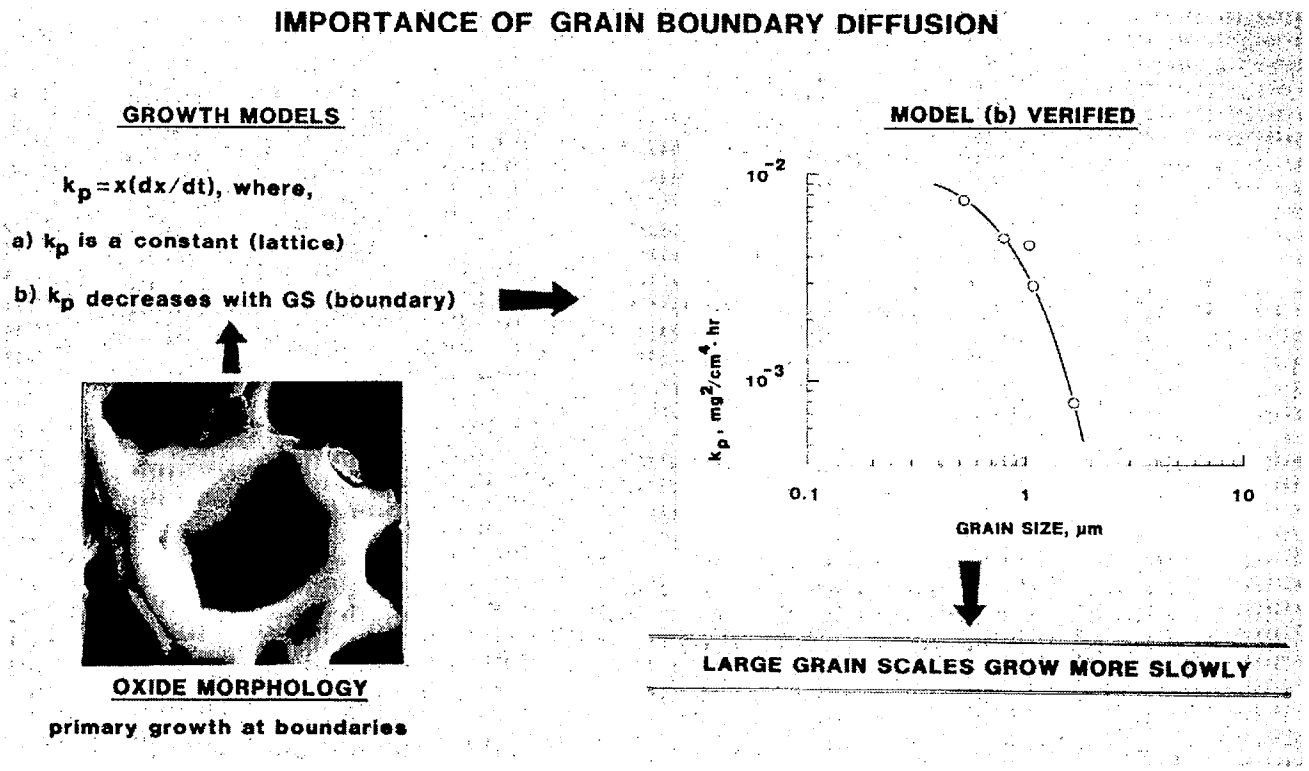

Figure 3

SEM MICROGRAPHS OF SPALLED Al_2O_3 SCALES

The rate of aluminum depletion controls the capability of an alloy or coating to be protected as a consequence of forming an aluminum oxide scale. In the case of an alloy of "infinite" thickness, aluminum oxide spallation is the depletion mechanism while the kinetics of subscale diffusion determines the capability for Al_2O_3 scale formation. Therefore, both spallation and subscale diffusion must be modeled to predict alloy environmental life. The scanning electron microscope micrographs of figure 4 illustrate two types of spalling behavior. The Ni-40Al alloy exemplifies spalling to exposed metal over a fraction of the surface area. The Ni-Cr-Al-Zr alloy displays spalling within the oxide scale over a fraction of the surface area.

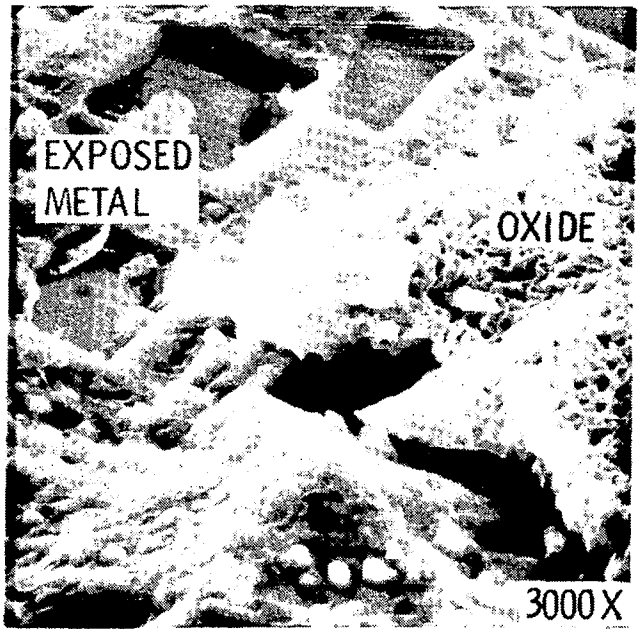

Ni-40 Al, 1200° C, 217 CYCLES

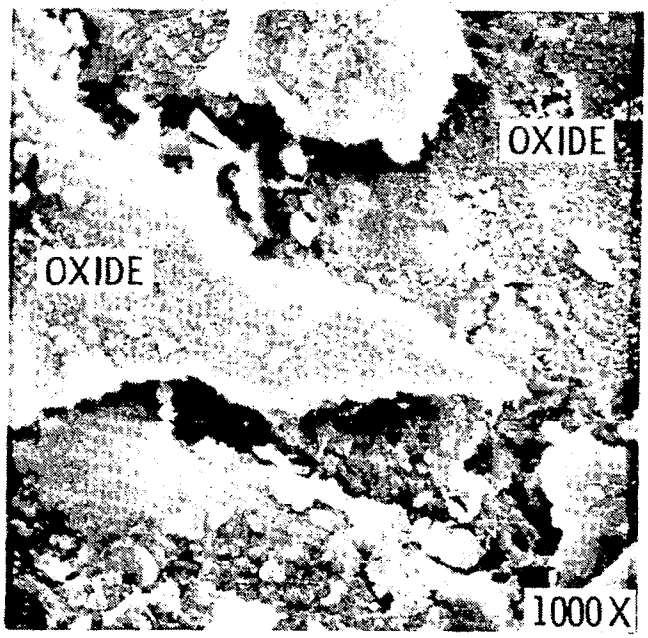

Ni-15Cr-24Al-0.3Zr, 1100° C, 500 CYCLES

Figure 4

CYCLIC OXIDATION VISUALIZATION

A cyclic oxidation model has been developed to predict aluminum depletion via spallation (C. E. Lowell, et al: Cyclic Oxidation of Superalloys. Proceedings of the International Conference on High-Temperature Corrosion, in press). In its simplest form, this model requires input data from isothermal oxidation tests only. The parameters required are the parabolic growth constant and a spalling fraction, Q. To model the actual behavior of the oxide surface, Q can be a constant spall fraction or can vary with oxide scale thickness. Also, Q can be set up to cover the case of spalling to bare metal or spalling within the oxide scale. For this detailed modeling, appreciable morphological data is also required. These various cases have been run using a computer model. Figure 5 illustrates three frames from a motion picture for a 400 segment model wherein the oxide spalls back 80 percent and with the spall fraction a function of scale thickness. At the end of the first heating cycle a uniform oxide scale has formed. Upon cooling, some oxide has spalled. After 100 cycles the surface structure becomes quite complex.

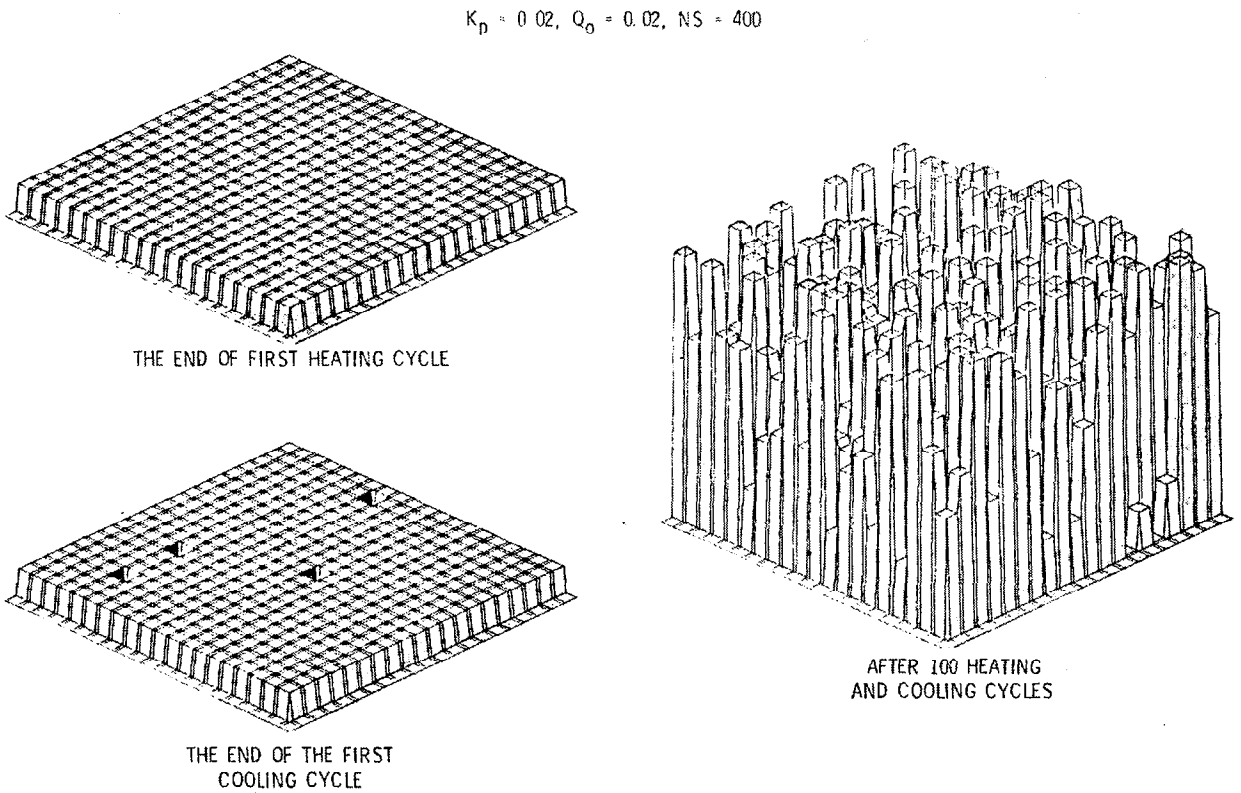

Figure 5

CYCLIC OXIDATION PREDICTIONS FOR TWO SPALL MODELS

Figure 6 illustrates the results of the Monte Carlo calculations for two spall models - bimodal as illustrated in figure 5 and uniform constant fraction of the scale. The parameters used in these calculations fit the oxidation behavior of the oxide dispersion strengthened alloy TD-NiCrAl at 1200° C. The outcome of the calculations does not show a significant difference between the models. This turns out to be true in all cases. This greatly simplifies the calculations and permits the use of simple isothermal test results to model cyclic oxidation. The model can readily account for cycle frequency. The output of the computation gives retained oxide, metal consumption and specific weight change as a function of time or cycles.

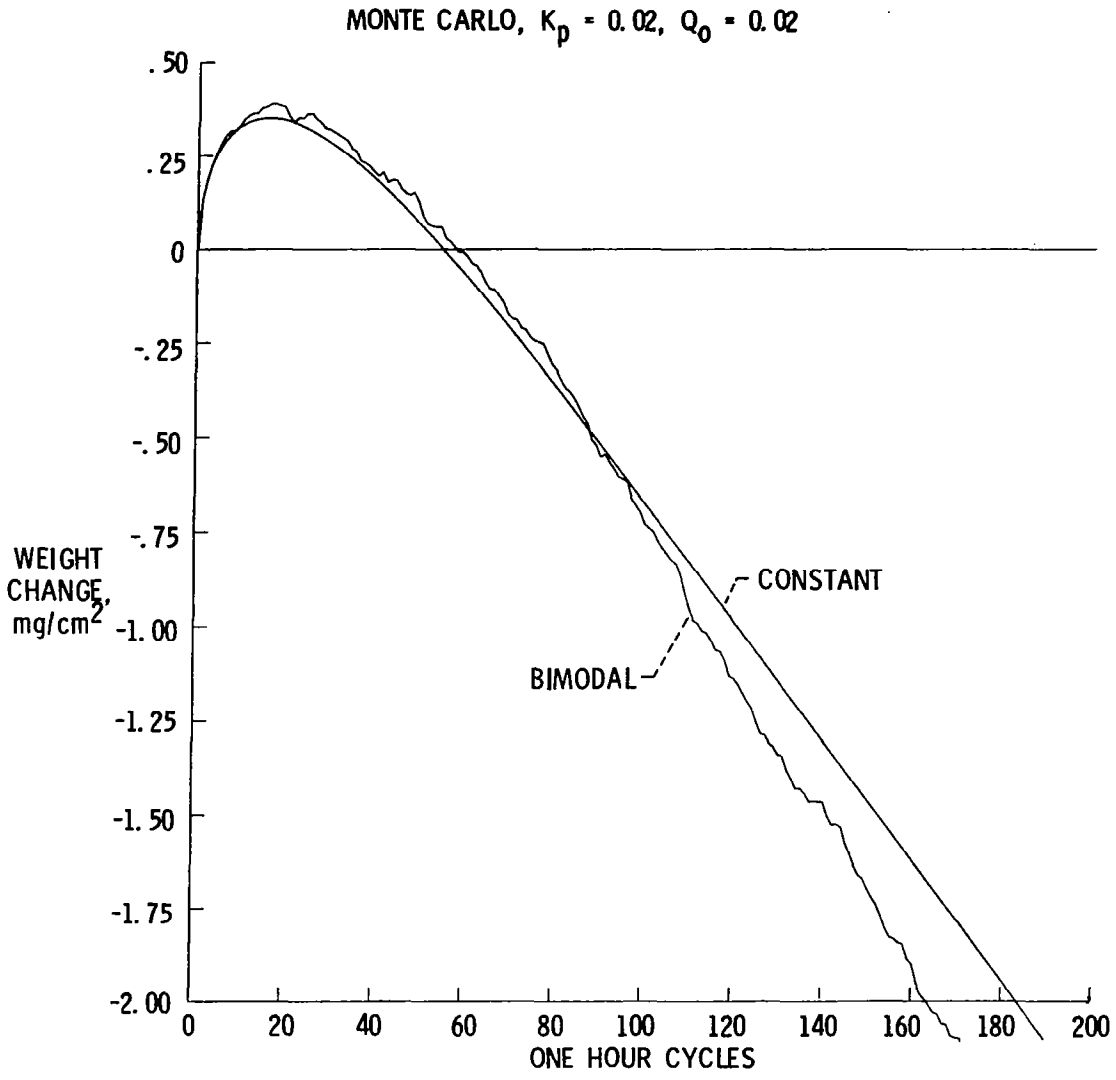

Figure 6

PREDICTIONS FROM ISOTHERMAL DATA AGREE WITH CYCLIC DATA

In figure 7, the results of a cyclic furnace oxidation experiment at 1200° C for an alumina forming NiCrAlZr alloy are compared with predictions from the cyclic oxidation model. The parameters for the model were determined from a short time isothermal test. Agreement is quite good out to 2500 1-hour cycles. At this point, a change in slope for the cyclic oxidation data is evident due to a change in the oxidation mechanism. At this point, the subscale can no longer provide aluminum at a sufficient rate and less protective oxides are formed.

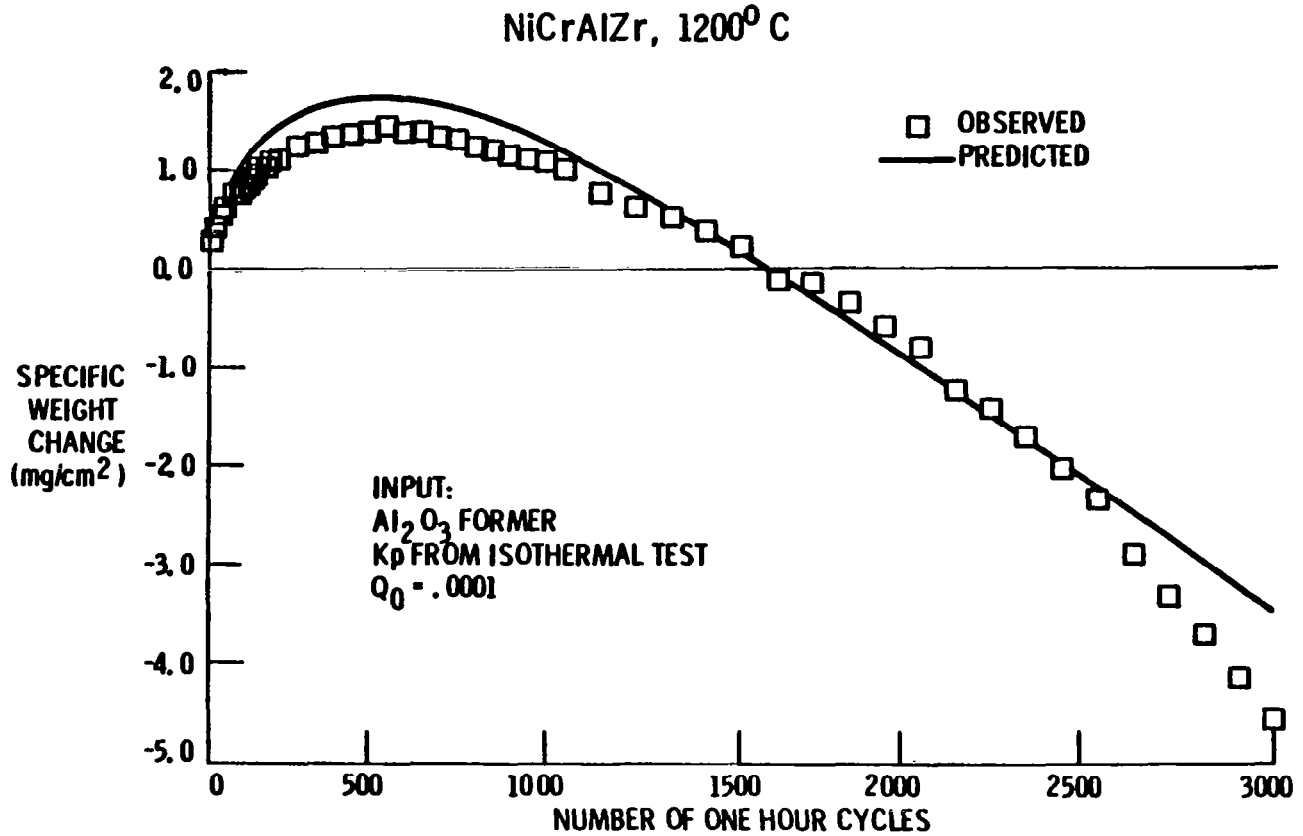

Figure 7

SUBSCALE DIFFUSION LIMITS OXIDATION LIFE

The key to predicting oxidation life then becomes integrating the cyclic oxidation model which accounts for aluminum depletion via oxide spallation with a subscale diffusion model which predicts the rate at which aluminum can diffuse to the surface. As illustrated in figure 8, at some critical concentration at the subscale surface, aluminum can no longer be supplied at a rate sufficient to meet the spalling demand and less protective oxides are formed. The subscale diffusion model has been developed (5) and it is being joined to the cyclic oxidation model.

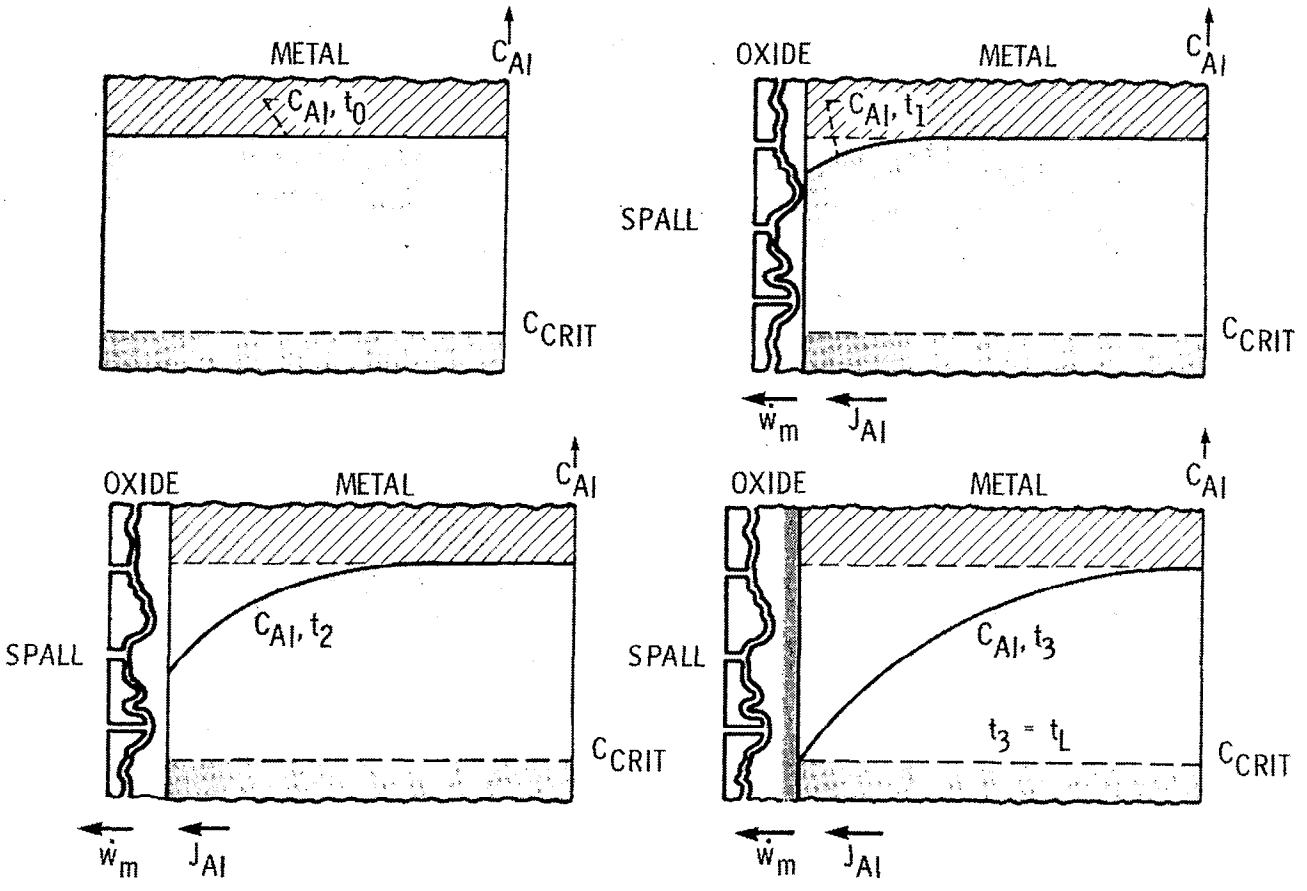

Figure 8

ENVIRONMENTAL AND SUBSTRATE REACTIONS DEGRADE COATINGS

In the case of finite metallic protective coatings, be they diffusionally formed aluminides or MCrAlY (M=Ni or Co) overlays, two distinct aluminum depletion mechanisms need to be dealt with - oxidation and interdiffusion. Figure 9 illustrates the nature and extent of these processes for a NiCrAlY overlay coating. Here the aluminum-rich NiAl phase in NiCrAlY has been over-etched so that it stands out. From these photomicrographs, it is evident that the diffusion reaction between the coating and substrate is of great importance. This has been documented for both aluminide (6) and overlay coatings (7). Also, some progress has been made toward controlling the kinetics of the reaction (7) and an effort to develop a diffusion model for coating life prediction is under way.

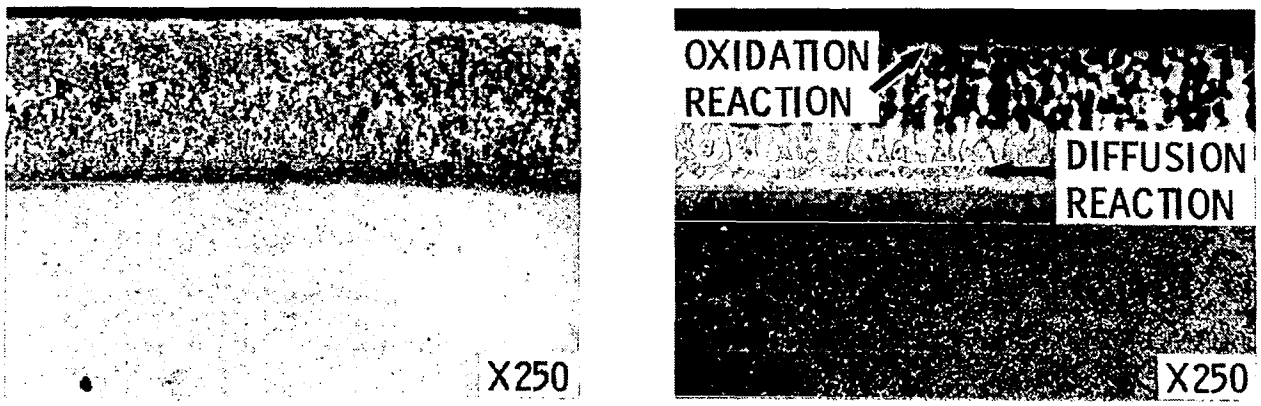

AS-DEPOSITED NiCrAlY COATING

AFTER 200 hr AT 2000^{0} F

Figure 9

SCHEMATIC OF THERMAL BARRIER COATING CONCEPT

Figure 10 introduces a new subject - thermal barrier coatings. Conventional airfoils in the early turbine stages of advanced aircraft gas turbines are cooled with air bled from the compressor. Such cooling and protection from the environment by a metallic coating are required to permit useful component lives while attaining the thermodynamic efficiency benefits of high cycle temperatures. The addition of a thin oxide ceramic layer to such an airfoil adds a significant thermal resistance - hence coatings of this class are called thermal barrier coatings (TBC). Such coatings are most commonly zirconia-based ceramics applied by plasma spraying. A typical microstructure is shown in figure 10. The function of the metallic coating has now been expanded to that of a bond coat. The addition of a ten mil ceramic layer can easily result in a 100° C reduction in metal temperature. This capability offers the options of improved component durability through metal temperature reduction or improved cycle efficiency through reduced cooling air use and/or higher cycle temperature (8).

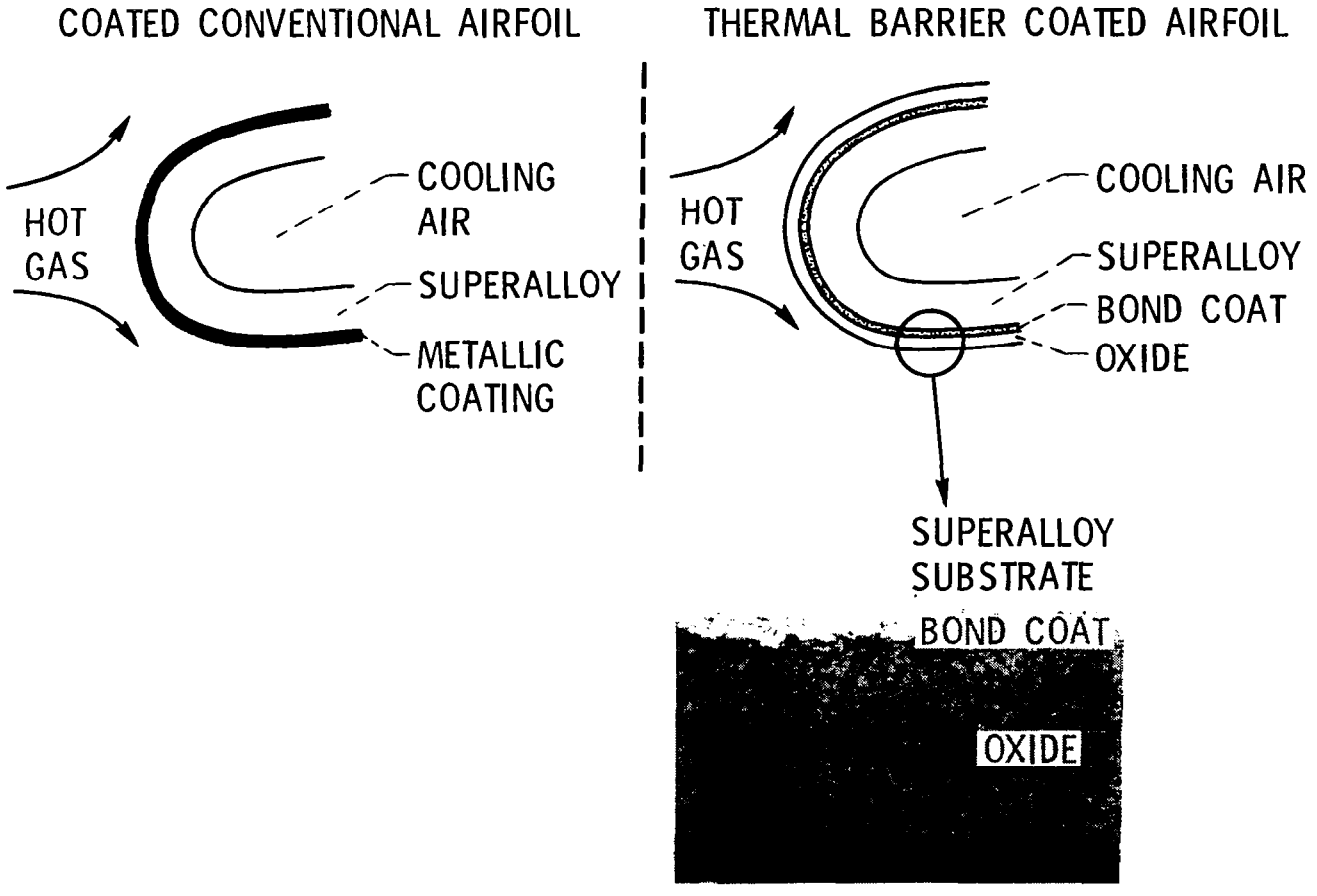

Figure 10

APPLICATIONS OF THERMAL BARRIER COATINGS

Figure 11 illustrates some current and projected future applications of TBC in aircraft gas turbines. Such coatings were introduced to JT8D combuster liners in the late 60's to extend life. They are now being introduced in an advanced JT9D as first stage vane platform coatings in conjunction with a revised cooling system wherein impingement/convection cooling is being used in place of film cooling (9). This results in reduced manufacturing cost, reduced cooling air use yielding higher SFC, and improved durability. Both of these applications involve non-critical static parts. In the late 80's, TBC may begin to be used on turbine airfoils. In initial applications, it is expected that the coatings will be used only to extend life. Our ultimate objective is to provide the research and technology base to permit their ultimate use on the leading edges of advanced aircraft gas turbine first stage blades for performance improvement.

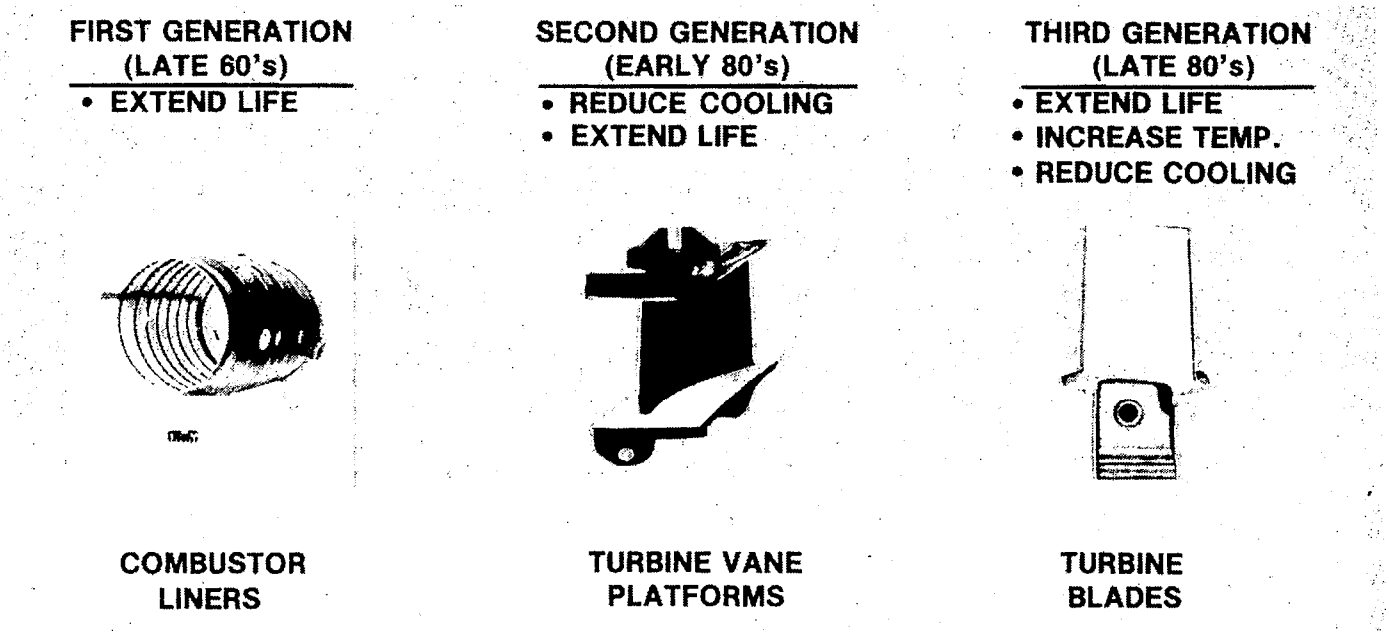

Figure 11

TYPICAL JT9D - 7E ENGINE TEST RESULTS OF TBC COATED BLADES

The current impetus for TBC research was derived from the successful test of two layer coatings on air-cooled first-stage blades in a J-75 research engine. The coatings tested survived 500 cycles between full power and flameout (10). A typical first-stage blade from a more recent and more severe test in a JT9D, figure 12, indicated that the ZrO_2 . 12 weight percent Y_2O_3/NiCrAlY coating is not yet ready as an add-on coating for first-stage blades. The coating was intact on the blade platform, suction surface, and most of the pressure surface. Analysis indicated that failures occurred in regions of combined high temperature and compressive stress (11).

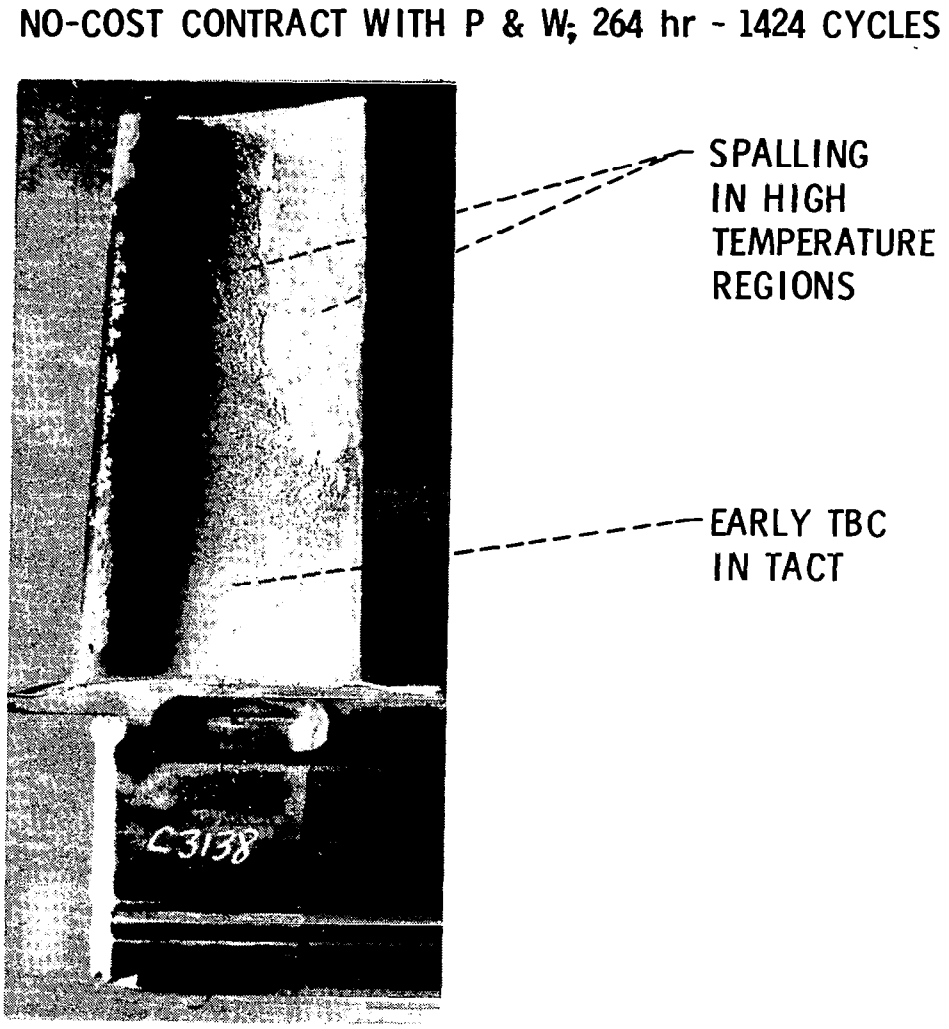

Figure 12

THERMAL BARRIER COATING PERFORMANCE

Based on the results of the JT9D test, it was clear that significant advances in TBC performance and in understanding of TBC behavior were required. The major thrusts of our effort are outlined in figure 13. In the areas of coating composition and structure, significant improvements in coating performance have been made and some of these will be discussed. The understanding of coating behavior in response to thermal stress and environmental degradation will provide the basis for correct design of coated components and will thus enable effective use of thermal barrier coatings.

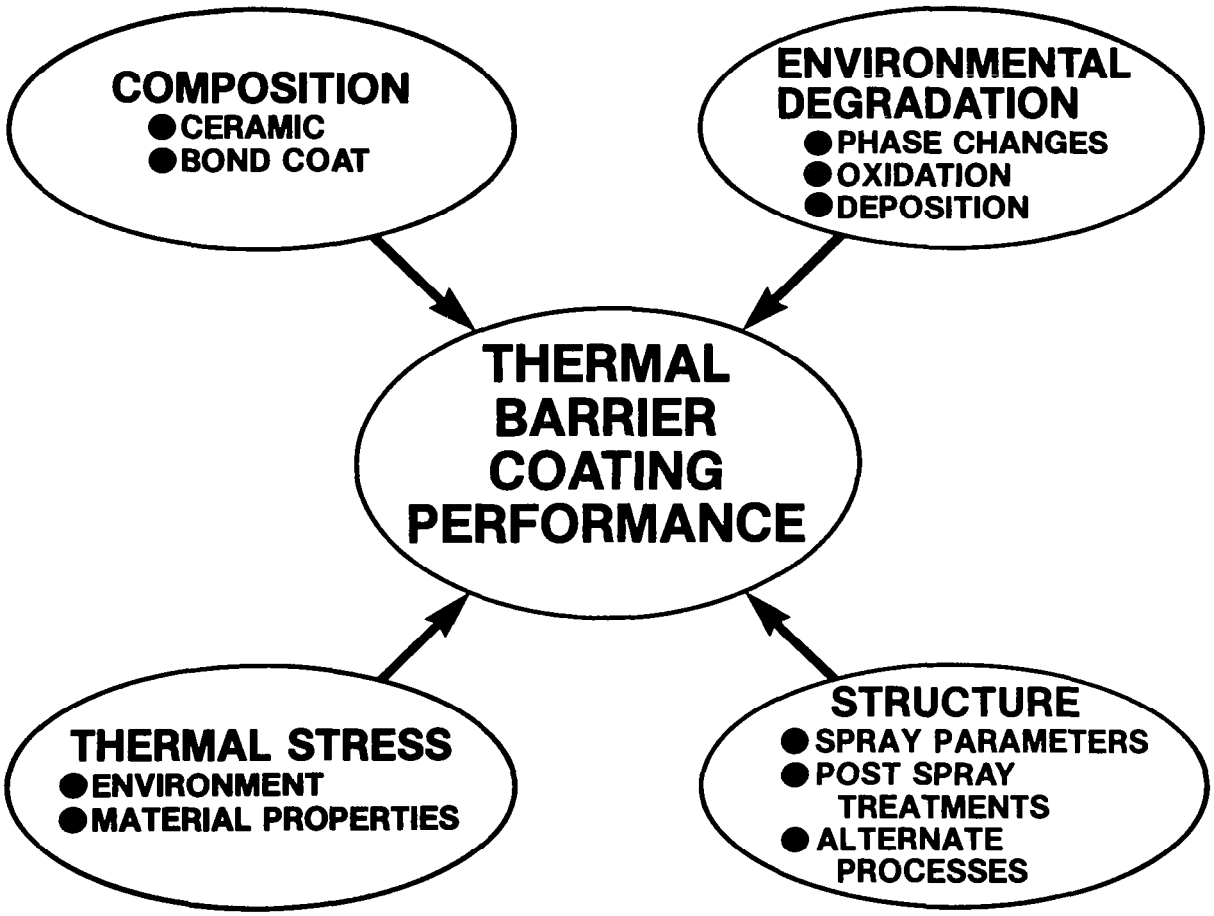

Figure 13

RESPONSE OF CERAMIC COATING TO STRESS OPPOSITE TO THAT OF BULK CERAMICS

One of the most important elements of understanding in both the processing of TBC and their use is the realization that conventional wisdom with regard to stresses in the ceramic does not apply. As illustrated in figure 14, TBC readily withstand tensile stresses which in this case have been induced by bending a coated metal strip around a mandrel. The coating is retained in tensile loaded areas of the convex surface. However, the ceramic has spalled from the concave surface where it was loaded in compression. The location of the failures are within the ceramic close to the bond coat-ceramic interface. This location is the weak link in ceramic coatings (12). The sensivity of ceramic coatings to compressive stress implies that processing should be carried out to minimize compressive residual stress (9). Also, components should be designed to minimize compressive stress generation during transients. However further investigation is required to find a solution to the longer term problem of stress relaxation at temperature and the implications on cooldown for a low coefficient of thermal expansion (CTE) TBC on a superalloy with higher CTE.

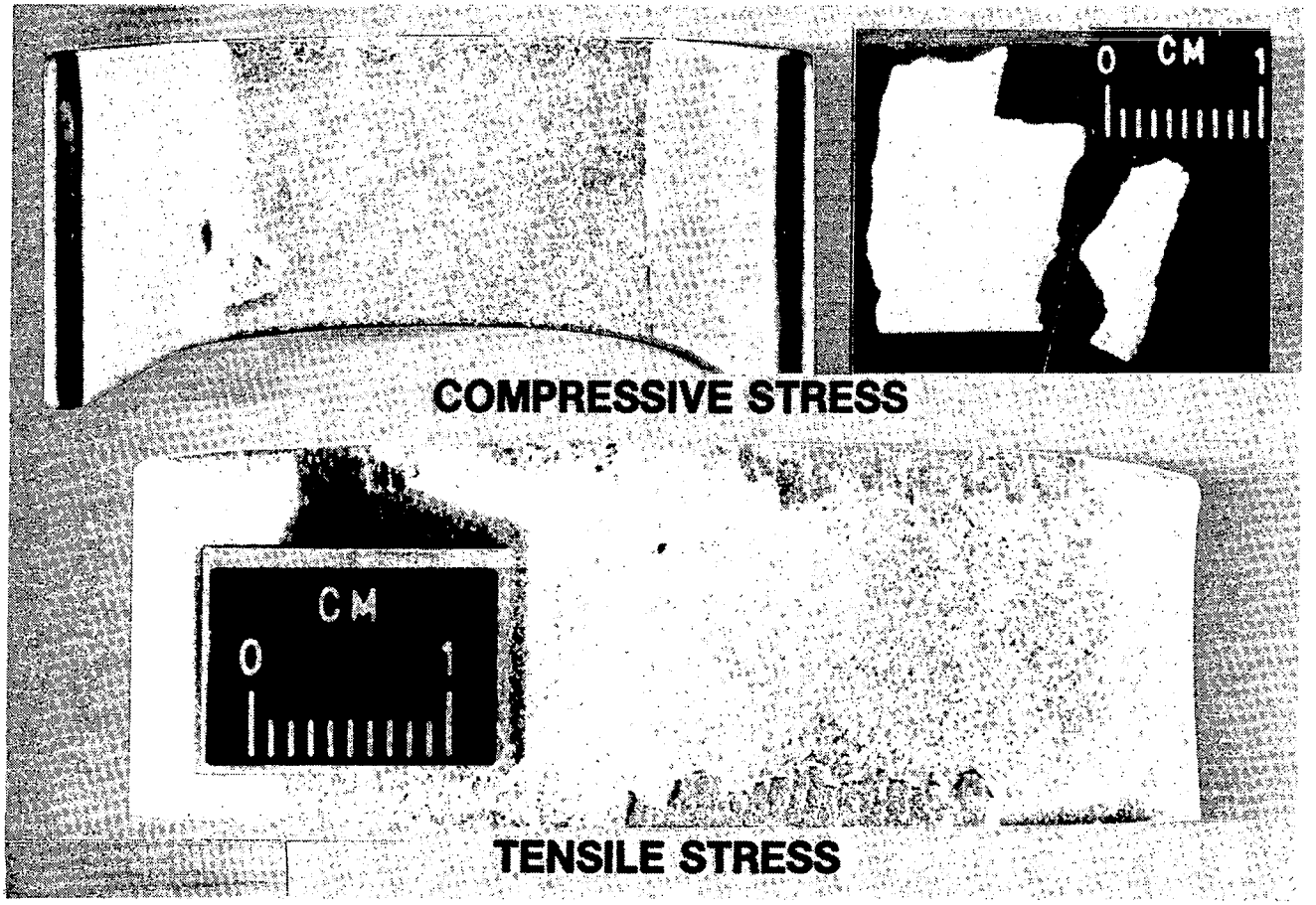

Figure 14

COATING COMPOSITION HAS IMPACT ON COATING LIFE

Early TBC research was oriented toward identifying zirconia based ceramics that were fully cubic phase stabilized rather than compositions that would undergo transformations between the cubic, tetragonal and monoclinic phases. The transformation from cubic or tetragonal to monoclinic was regarded as particularly undesirable because of its disruptive volume expansion. The early NASA ZrO_2 - 12 weight per cent Y_2O_3 coating fell into the category of a fully cubic phase stabilized zirconia (13). An investigation of the effect of yttria stabilizer level on ZrO_2 - Y_2O_3 TBC life revealed that the most durable coatings were obtained with partially stabilized zirconias (about 6 weight per cent yttria) applied to low yttrium NiCrAlY bond coats (14). The 4 weight per cent yttria stabilized zirconia (YSZ) composition was undesirable due to excessive monoclinic phase formation. In hot corrosion-inducing environments, 8 weight per cent YSZ has proven to be more durable than 6 weight per cent YSZ (15). Therefore, the 6 to 8 weight per cent range has been the focus of recent research. (See fig. 15.)

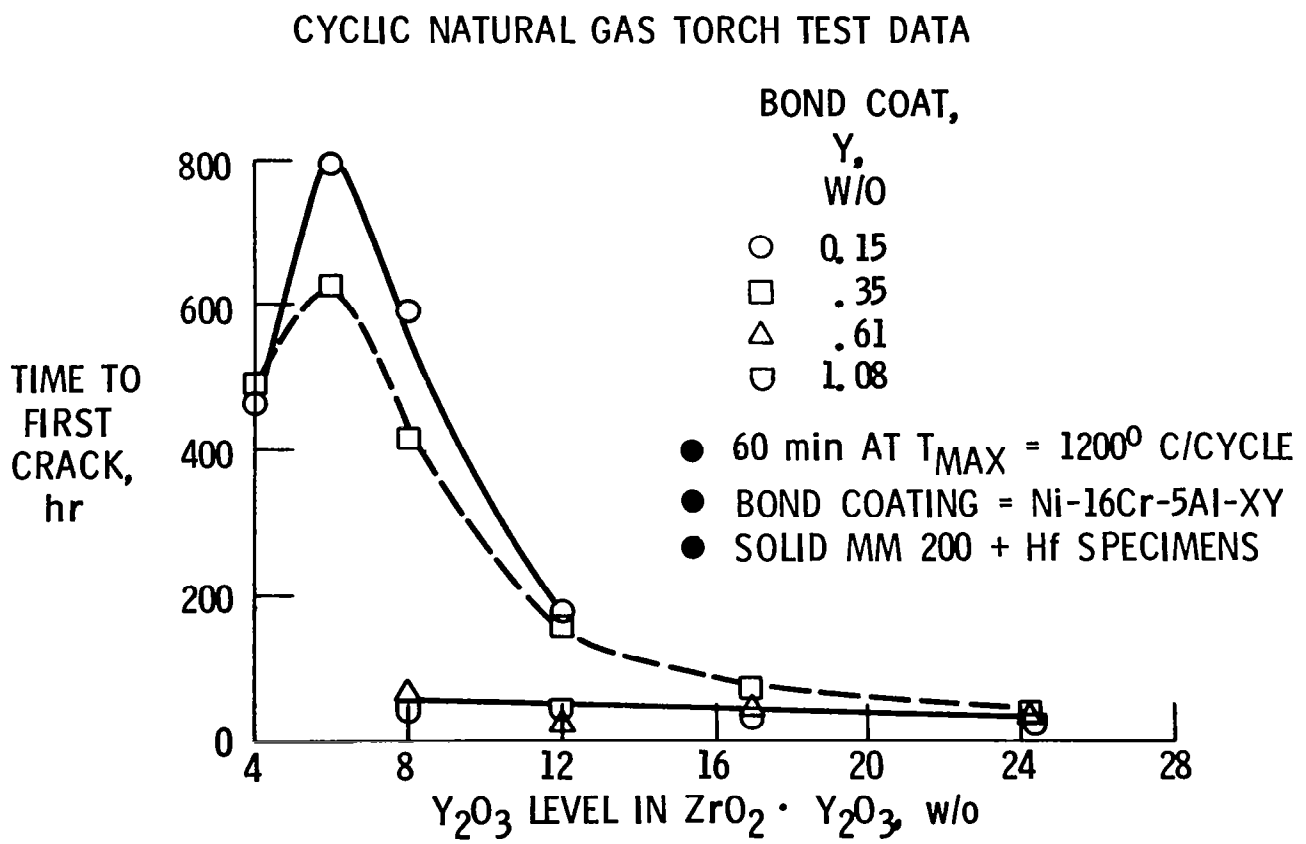

Figure 15

TBC FAILURE MECHANISMS

Thermal barrier coatings can fail due to thermal stress or due to thermally activated processes such as creep of the ceramic or bond coat, oxide sintering, or bond coat oxidation. These latter processes may degrade the coating to the point where thermal stress is the mechanism responsible for ceramic spallation. Separating these two major categories of failure mechanisms has proven to be a difficult process. However, by varying the length of the thermal cycle, it is possible to project two life curves for the pure failure mechanisms as shown at the upper left of figure 16. Early results in Mach 0.3 burner rig tests for a TBC with an oxidation prone Ni-16Cr-6Al-0.3Y bond coat seemed to indicate that thermal stress was responsible for coating failure (16). With more oxidation resistant bond coats, a mixed failure mode was identified (17), but the controlling mode could not be pinned down. By going to cycles of short duration (30 seconds) so that thermal stress was the only permissible failure mechanism, it was shown that thermal stress alone can not induce failure in the Mach 0.3 burner rig test (fig. 16). In the short cycle test, the coating survived 10,000 cycles without failure. However, a few cycles of longer duration, or pre-exposure of the coating in air for about 20 hours at 1250° C resulted in sufficient thermal degradation to cause coating failure (18). In cyclic thermal exposures at higher rates of heat input, as might be found in an engine, the role of thermal stress vs thermally activated processes remains to be determined. Based on the JT9D test and subsequent analysis, it is postulated that thermal stress may become dominant as the heat flux increases. A high pressure burner rig, soon to be constructed at Lewis, will be used to determine TBC failure mechanisms at advanced engine conditions.

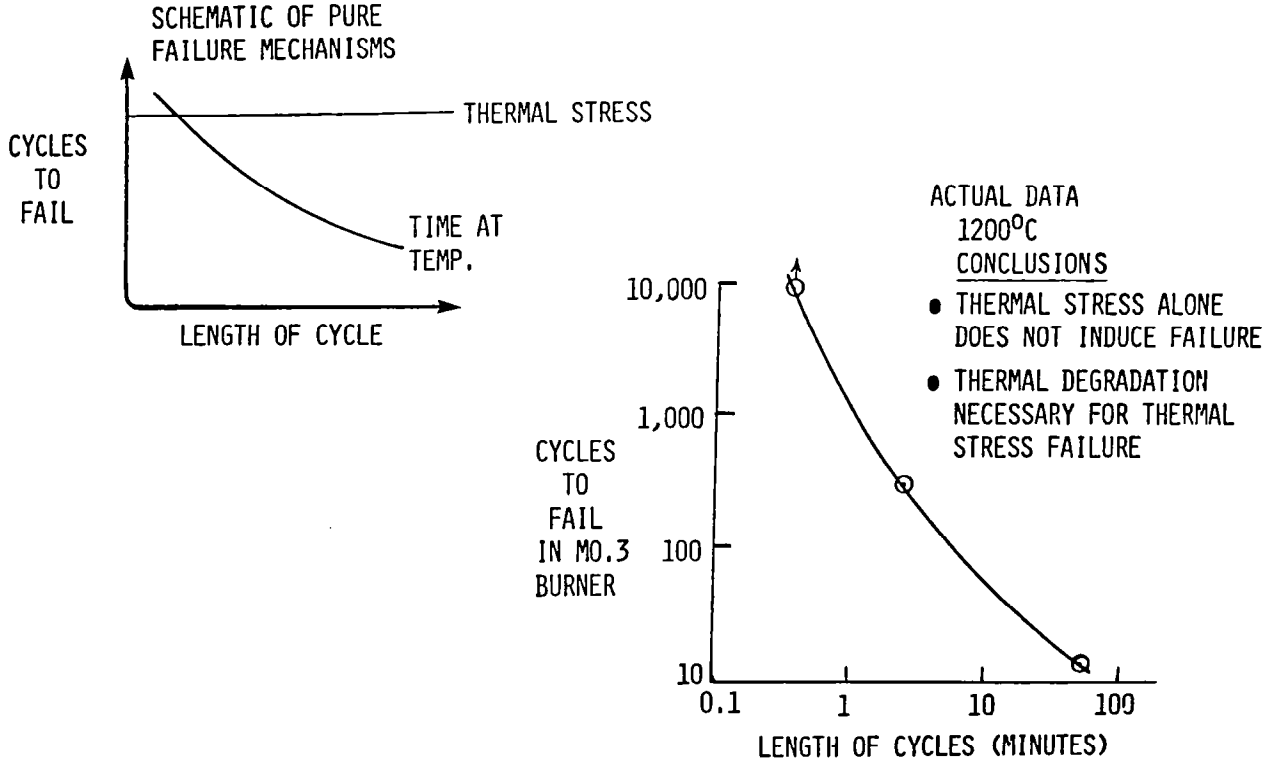

Figure 16

LIFE EXTENSION FOR THERMAL BARRIER COATINGS (TBC)

As pointed out earlier, the bond coat plays a dual role in a TBC. It provides oxidation and hot corrosion protection for the superalloy substrate while providing a good mechanical bond between the substrate and ceramic coating. The oxidation of the bond coat has been identified as a key potential failure mechanism for TBC (17,18). Significant improvements to the durability of TBC have been made through the use of more oxidation resistant bond coat compositions combined with improved plasma spray processing (17,19,20) as illustrated in figure 17(17). The improved compositions have high Cr and Al contents to provide a greater reservoir of protective oxide scale formers. Processing improvements include higher power levels and additions of hydrogen to the arc gas. Further improvements through low pressure plasma spray processing (21) can be anticipated.

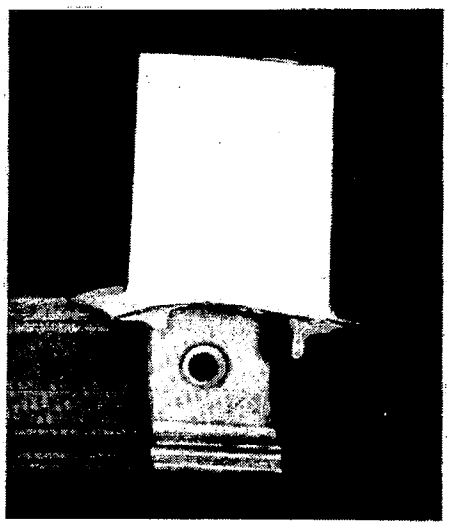

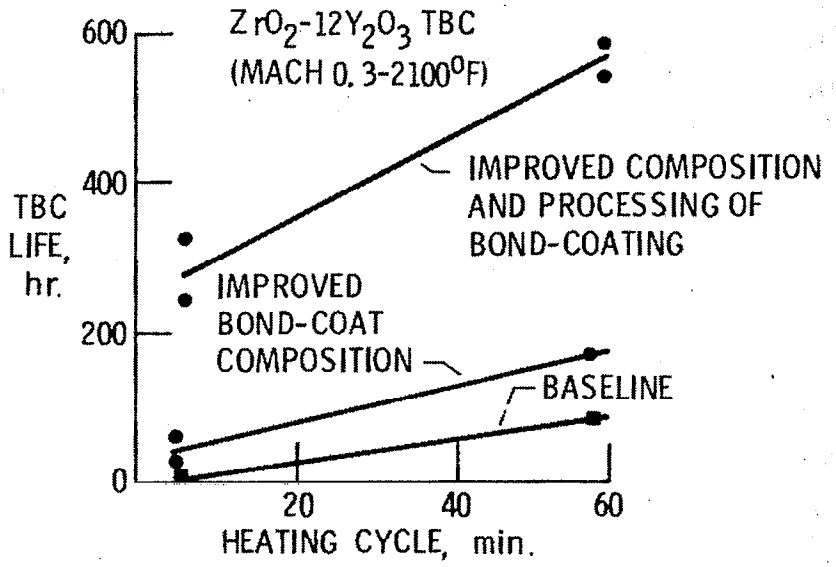

MATERIAL/PROCESS IMPROVEMENTS PRODUCE
• 10X LIFE IMPROVEMENT
OR
• 100°C TEMPERATURE INCREASE
OVER CURRENT THERMAL BARRIER COATINGS

Figure 17

THERMAL BARRIER COATING (TBC) TECHNOLOGY TRANSFER

Development of advanced technology, such as TBC, by NASA does little good unless it can be effectively transferred to industry. Lewis has entered into a number of cooperative agreements (contractual or informal) with various industrial concerns to transfer TBC to the user by providing hands-on experience. The results of some of these ventures are reported in the literature (22,23). Figures 18 and 12 illustrate some of the ventures in which we have participated, and the results and benefits obtained.

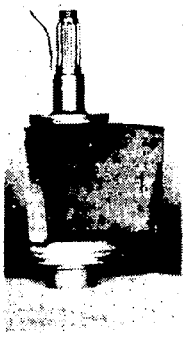

ADVANCED GAS TURBINE VANES

- APPLICATION OF TBC TO DDA/ATEGG VANES PREVENTED CRACKING AND MELTING

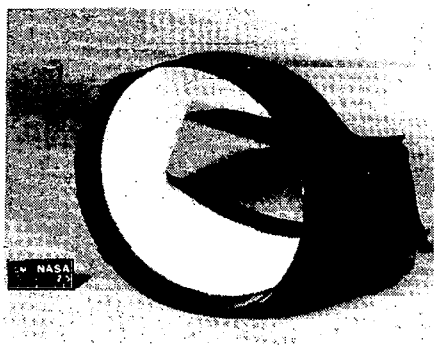

GAS TURBINE COMBUSTOR TRANSITION SECTIONS

- NASA TBC ADHERED PREVENTING WARPING OF TRANSITION SECTIONS

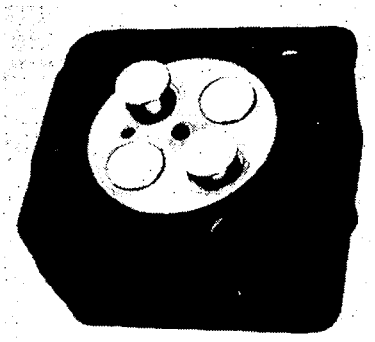

DIESEL ENGINE HEAD AND VALVES

- TBC ADHERED AND PROVIDED SOME OF THE REQUIRED INSULATION

Figure 18

REFERENCES

1. Grisaffe, S. J.; Lowell, C. E.; and Stearns, C. A.: High Temperature Environmental Effects on Metals. Risk and Failure Analysis for Improved Performance and Reliability, J. J. Burke and V. Weiss, eds., Plenin Publishing Corp., 1980, pp. 225-242.

2. Stearns, C. A.; Kohl, F. J.; and Rosner, D. E.: Combustion System Processes Leading to Corrosive Deposits. NASA TM-81752, 1981.

3. Merutka, J. P.: Progress in Protective Coatings for Aircraft Gas Turbines - A Review of NASA Sponsored Research. NASA TM-82740, 1981.

4. Smialek, J. L.: Microstructure of Al_2O_3 Scales Formed on NiCrAl Alloys. NASA TM-81676, 1981.

5. Nesbitt, J. A.: Solute Transport During the Cyclic Oxidation of Ni-Cr-Al Alloys. NASA CR-165544, 1982.

6. Smialek, J. L.; and Lowell, C. E.: Effects of Diffusion on Aluminum Depletion and Degradation of NiAl Coatings. J. Electrochem. Soc., Vol. 121, 1974, pp. 800-805.

7. Gedwill, M. A.; Glasgow, T. K.; and Levine, S. R.: A New Diffusion-Inhibited Oxidation-Resistant Coating for Superalloys. NASA TM-82687, 1981.

8. Levine, S. R.; Miller, R. A.; and Hodge, P. E.: Thermal Barrier Coatings for Heat Engine Components. SAMPE Quarterly, Vol. 12, 1980, pp. 20-26.

9. Sheffler, K. D.; and Graziani, R. A.: JT9D Thermal Barrier Coated Vanes. NASA CR-167964, 1982.

10. Liebert, C. H.; Jacobs, R. E.; Stecura, S.; and Morse, R.: Durability of Zirconia Thermal-Barrier Ceramic Coatings on Air-Cooled Turrbine Blades in Cyclic Jet Engine Operation. NASA TM X-3410, 1976.

11. Sevcik, W. R.; and Stoner, B. L.: An Analytical Study of Thermal Barrier Coated First Stage Blades in a JT9D Engine. NASA CR-135360, 1978.

12. Levine, S. R.: Adhesive/Cohesive Strength of a ZrO_2-12 w/o Y_2O_3/ NiCrAlY Thermal Barrier Coating. NASA TM-73792, 1977.

13. Stecura, S.: Two-Layer Thermal Barrier Coating for High Temperature Components. Ceramic Bulletin, Vol. 56, 1977, pp. 1081-1089.

14. Stecura, S.: Effects of Compositional Changes on the Performance of a Thermal Barrier Coating System. NASA TM-78976, 1978.

15. Hodge, P. E.; Miller, R. A.; and Gedwill, M. A.: Evaluation of Hot Corrosion Behavior of Thermal Barrier Coatings. NASA TM-81520, 1980.

16. McDonald, G.; and Hendricks, R. C.: Effect of Thermal Cycling on ZrO_2-Y_2O_3 Thermal Barrier Coatings. NASA TM-81480, 1980.

17. Gedwill, M. A.: Burner Rig Evaluation of Thermal Barrier Coating Systems for Nickel-Base Alloys. NASA TM-81683, 1981.

18. Miller, R. A.; and Lowell, C. E.: Failure Mechanisms of Thermal Barrier Coatings Exposed to Elevated Temperatures. Thin Solid Films, Vol. 95, 1982, pp. 265-273.

19. Stecura, S.: Effects of Yttrium, Chromium, and Aluminum Concentrations in Bond Coatings on the Performance of Zirconia Yttria Thermal Barriers. NASA TM-79206, 1979.

20. Stecura, S.: Effects of Plasma Spray Parameters on Two-Layer Thermal Barrier Coating System Life. NASA TM-81724, 1981.

21. Pennisi, F. J.; and Gupta, D. K.: Tailored Plasma Sprayed MCrAlY Coatings for Aircraft Gas Turbine Applications. NASA CR-165234, 1981.

22. Liebert, C. H.; and Stepka, F. S.: Industry Tests of NASA Ceramic Thermal Barrier Coatings - for Gas Turbine Engine Applications. NASA TP-1425, 1979.

23. Liebert, C. H.; and Levine, S. R.: Further Industrial Tests of Ceramic Thermal-Barrier Coatings. NASA TP-2057, 1982.